ORIGINAL RESEARCH PAPER

Volume-7 | Issue-11 | November-2018 | PRINT ISSN No 2277 - 8179

INTERNATIONAL JOURNAL OF SCIENTIFIC RESEARCH

MRI EVALUATION OF THE SELLAR, PARA-SELLAR AND SUPRA-SELLAR LESIONS.

Radiodiagnosis

Dr. Nilesh Chaudhari Associate Professor, Department of Radio-diagnosis, Dr.Vasantrao Pawar Medical College Hospital & Research Centre, Nashik, Maharashtra, India.

Dr. Prerit J. Sharma* Junior Resident (III), Department of Radio-diagnosis, Dr.Vasantrao Pawar Medical College Hospital & Research Centre, Nashik, Maharashtra, India. *Corresponding Author

Dr. Priti Komatwar Junior Resident (II), Department of Radio-diagnosis, Dr.Vasantrao Pawar Medical College Hospital & Research Centre, Nashik, Maharashtra, India.

ABSTRACT

Background : The sellar region is a relatively complex anatomical area surrounding the pituitary gland and contains crucial neuro-vascular structures. Pituitary lesions although relatively infrequent, have a significant impact on the quality of life. The main aim of this study is to discuss the crucial anatomy and identification of the characteristic features of the important pathological lesions involving the sellar, parasellar and suprasellar regions. This study also emphasizes on the role of advanced imaging modalities like Magnetic Resonance (MR) imaging in evaluation of pituitary-hypothalamic axis lesions. Magnetic resonance imaging has been proven to be the imaging modality of choice in the neuroimaging assessment of most pathology occurring at the skull base.

Materials and Methods: MRI brain of 59 patients with varying clinical symptoms was performed on 1.5-T MR system using a dedicated head coil.

Purpose: To illustrate imaging features of various sellar, parasellar and suprasellar lesions using MRI.

Results: A total of 59 patients in a span of 2 years were compiled and analyzed, comprising of 34 cases of macroadenomas, 10 cases of juxta/parasellar meningiomas and 9 cases of craniopharyngiomas. Majority of patients in this study belonged to the age group 31-40 years. Females predominated in this study constituting 60% of the total study population. Commonest overall sellar/parasellar/suprasellar mass on MRI was pituitary macroadenoma (34%).

Conclusion: MRI is an excellent modality for classifying and evaluating the different sellar, parasellar and suprasellar lesions. Recent advanced MRI tests aids in characterization and narrowing the differential diagnosis, for definitive diagnosis, still histologic tissue evaluation is needed for uncommon and tumors with atypical presentation. Thus by providing complete information, MRI helps in better management and prognosis of these patients.

KEYWORDS

Magnetic Resonance Imaging (MRI), neoplasms, neuroimaging, parasellar, pituitary, sellar, and suprasellar lesions.

INTRODUCTION

Pituitary gland plays a very crucial role in the overall growth and metabolism of the body. It also regulates the reproductive functions. The surrounding area i.e. the sellar and parasellar region is an anatomically complex area that acts as an important junction for critical adjacent structures[1]. The anterior lobe of the pituitary gland secretes six hormones: thyroid-stimulating hormone (TSH), previously adrenocorticotropic hormone (ACTH), follicle-stimulating hormone (FSH), leuteinizing hormone (LH), growth hormone (GH), and prolactin (PRL). The posterior pituitary gland secretes vasopressin and oxytocin.

A spectrum of diseases that affect the pituitary-hypothalamic axis also have profound clinical, endocrinological and neurological consequences that have a major impact over the overall quality of life. These conditions can be classified as physiological, congenital/ developmental, neoplastic, infectious, inflammatory and post-traumatic. Various neoplastic conditions include pituitary adenoma/ apoplexy, hypothalamic glioma, craniopharyngioma, rathke cleft cyst, germinoma, teratoma, metastasis, leukemic infiltration, lymphoma, and Langerhans cell histiocytosis. Infectious and inflammatory causes include tubercular/ lymphocytic hypophysitis, sarcoidosis, and Wegener's granulomatosis. Traumatic causes include postoperative sella or transection of the pituitary stalk.

Accurate diagnosis with differentiation of these lesions is thus essential for safe and effective management of the condition. MRI is the imaging modality of choice in the evaluation of pituitary tumors. Dynamic MR Imaging plays a very important role in the evaluation of pituitary adenomas, particularly in accurate delineation of those microadenomas with no contour abnormality, and in post operative evaluation in cases of residual / recurrent lesions[2]. It is also useful in the assessment of macroadenoma [2].

AIMS AND OBJECTIVES

1. To study the characteristic MRI features of sellar, parasellar and suprasellar lesions.
2. To identify and classify sellar, parasellar and suprasellar lesions.

MATERIALS AND METHODS

This study was conducted over a period of 2 years from June 2016 to June 2018 with due permission from the ethics committee. A total of 59 patients with suspected sellar, parasellar and suprasellar lesions referred to the Department of Radio-diagnosis at Dr. Vasantrao Pawar Medical College, Hospital and Research centre, Nashik were subjected to dynamic pituitary MR imaging. The clinical and demographic data were recorded after due consent to correlate the findings. The patients who have already undergone surgical resection were not included in the study.

Follow up was obtained for histopathological diagnosis, laboratory investigations and follow up imaging studies wherever possible except for some cases where follow up could not be obtained due to migratory rural population and where diagnostic findings were confirmatory and additional supportive diagnostic test was not required.

MRI TECHNIQUE

All the MRI scans were done on 1.5-T magnet MR system (Siemens magneto Essenza) using dedicated brain coil.

All had a standard protocol, which included pre and post-contrast T1-weighted sequences in coronal and sagittal planes at 3-mm thickness with 0-mm skip. All had sagittal T2-weighted volume acquisition performed using 0.4-mm thickness, with coronal reformatted images. Axial postcontrast 1.4-mm volume acquisition with coronal and sagittal reformatted images were also available for all studies. All were obtained with the administration of intravenous gadolinium contrast at 0.1 mm/kg body weight (0.2 ml/kg), with a maximum dose of 20 ml.

Initially, the study was commenced with a pre-contrast protocol. In this protocol, T1 and T2 spin echo sagittal and coronal T1 and T2 weighted

images were obtained.

Following the routine scans, dynamic scan menu was initialized and scanning commenced with T1 TSE weighted images obtained in the coronal plane using thin 3 mm sections. The FOV was maintained at 19 cm. Fifteen dynamic sequential images in five fixed sections in the coronal plane over a period of 180 seconds were obtained during slow intravenous gadolinium administration of a preloaded10 ml syringe over a period of fifteen seconds with a 21 gauge butterfly needle placed in the antecubital fossa. Saline flushing with 5 ml was performed before and after administration.

The sequence protocol of 15 dynamic scan of three slices in the coronal plane using a TSE sequence (TR = 540 msec: TE = 13 msec) was strictly applied. The objective was to obtain the most spatially detailed images of the anterior lobe of the pituitary gland in the coronal plane, with the best possible signal noise ratio in the shortest period.

RESULTS

Total 59 patients referred to our department in a span of 2 years were examined and their MRI features were studied with the aim of describing extra-axial lesions, comprising of 34 cases of macroadenomas, 10 cases of juxta/parasellar meningiomas and 9 cases of craniopharyngiomas. The salient observations are as follows:

- Majority of patients in this study belonged to the age group 31-40 years (Table 1).
- Females predominated in this study constituting 60% of the total study population (Table 2).
- Commonest overall sellar/suprasellar mass on MRI was pituitary macroadenoma (34%). The second most common tumoral lesion detected in our study was meningioma which constituted 17% of total patients (Table 3).
- Out of 20 MRI diagnosis of macroadenoma, 2 cases turned out to be other lesions on HPE, i.e. 1 meningiomas and 1 craniopharyngiomas.
- Out of 10 MRI diagnosis of meningioma, 2 cases turned out to be macroadenoma on HPE.

DISCUSSION:

Embryology :

The pituitary gland development is a complex process with involvement of the development of diencephalon and the primitive oral stomodeum[3].

The adenohypophysis derives from a diverticulum that arises from the primitive Rathke's pouch, which originates rostral to the oropharyngeal membrane and projects toward the central skull base , around the 4th and 5th week of gestation[4][5].

It begins at approximately 24 days of gestation, an ectodermal outpouching of stomodeum forms the Rathke's pouch which eventually grows dorsally. The connection of Rathke's pouch to the stomodeum is eventually lost with subsequent formation of a sac that adheres to the diverticulum, which loses its connection to the oral cavity and forms a sac which continues to differentiate into the adenophyophysis. Rathke's pouch usually regresses during early fetal development. Occasionally, its remnant persists into the postnatal life and gives rise to a macroscopic cyst, the Rathke cleft cyst[6].

The anterior wall of the sac gets filled with cells and forms the pars distalis. A persistant small cleft between the anterior and posterior wall, forms the pars intermedia.Superior growth of a small infundibular process is responsible for the development of the pars tuberalis. The posterior diencephalic tissue differentiates into the neurohypophysis.

Anatomy :

Sella turcica is a saddle-shaped concavity in the sphenoid body with a component from the basiocciput where the pituitary gland is situated. The sphenoid body is in the midline and is anterolateral and superior extensions are the greater wings which also form the anteromedial aspects of the middle cranial fossa. The carotid sulci are located above their attachment to the sphenoid body lodging the internal carotid arteries and lateral cavernous sinuses. Anteriorly, it is bounded by the tuberculum sella, posteriorly by the dorsum sella and the posterior clinoid processes. The anterior clinoid processes of the lesser wing of the sphenoid are lateral to the tuberculum sella and project posteriorly while the connection between the two lesser wings is the planum sphenoidale. The floor of the sella is formed by the roof of the sphenoid sinuses, and any pathology affecting the architecture of the sinuses can result in alteration of the floor of the sella.

The sellar region is bounded by the suprasellar cistern and its contents, a reflection of the inner dural layer called diaphragmasellae from which the infundibulum passesand hypothalamus superiorly; the paired cavernous sinuses laterally, sphenoid sinus anteroinferorly and the dorsum sella and brainstem posteriorly.

Bilateral cavernous sinuses extend from the petrous segment of the temporal bone to the orbit and contain CN III (Oculomotor), IV (Trochlear), V1 (Ophthalmic division of the trigeminal nerve), V2 (Maxillary division of the trigeminal nerve) and VI (Abducens). The most medial structures in the cavernous sinuses are the internal carotid artery and CN VI. Bilateral Meckel's caves through which mandibular division of the trigeminal nerve (V3) exits are infero-lateral to each of the cavernous sinuses.

The pituitary gland has two anatomically and functionally distinct lobes: the anterior lobe (adenohypophysis) and the posterior lobe (neurohypophysis).The anterior lobe comprises 75% of volume of the gland and consists of pars tuberalis (part of the infundibular stalk and median eminence of hypothalamus), pars intermedia (a vestigial structure and common site for developmental cyst) and pars distalis (forms most part of intrasellar adenohypophysis)[7].

At birth, the gland is physiologically enlarged with a corresponding concave superior margin, with eventually flattens with age. In preterminfants, the gland is taller than in normal-term infants as a result of reduced insulin-like growth factor 1 and higher levels of growth hormone in premature infants and measures between 2 to 6 mm in height during childhood and up to 10 mm or slightly higher at puberty[8][9].

A useful guide to the gland's height in relation to age is “Elster's rule” of 6,8,10,12: 6 mm for infants and children, 8 mm in men and postmenopausal women, 10 mm in women of childbearing age and 12 mm for women in late pregnancy or postpartum women[10].

The pituitary stalk has a normal thickness of 2 mm, and it should not exceed a maximum of 4 mm or the width of the basilar artery. The hypothalamus and the pituitary gland are functionally and physiologically interlinked contiguous structures and often referred to as the hypothalamic-pituitary axis[11].

The anterior pituitary lobe receives its blood principally from the hypophyseal-portal system, which also serves as a pathway for release of hypothalamic hormones.

The hormones produced and secreted by the anterior lobe include growth hormone (GH), adrenocorticotropic hormone (ACTH), prolactin (PRL), thyroid stimulating hormone (TSH), luteinizing hormone (LH), and melanocyte-stimulating hormone (MSH).

The posterior pituitary lobe, infundibular stalk, supraoptic, and paraventricular hypothalamic nuclei form the neurohypophysis. The oxytocin and vasopressin, synthesized in the hypothalamus, are transported along the hypothalamo-hypophyseal tract to the posterior lobe and stored there.

At birth, both the anterior and posterior pituitary gland have high signal intensity on T1-weighted images. The anterior pituitary progressively decreases in signal intensity on T1-weighted images with signal drop to near iso-intensity with the posterior pons by 6 weeks of age[9][12].
The posterior pituitary gland retains its high signal intensity on T1-weighted images throughout adulthood, with several papers supporting that this high signal results from neurosecretory granules or the protein neurophysin.

Neurosecretory vesicles are responsible for high signal intensity of the posterior pituitary lobe.

The absence of high signal is often associated with central diabetes insipidus or compressive pituitary gland lesions[13][14].

Above the sellar region lies the suprasellar cistern through which traverse this area, including the circle of Willis, optic nerves and optic chiasm, hypothalamus, pituitary infundibulum, and the infundibular

and suprachiasmatic recesses of the third ventricle.

Plain skull radiographs were previously used to evaluate the sellar and parasellar lesions but they have been proven poor at delineating soft tissues as the radiographic size of sella is not a sensitive indicator of any pituitary gland pathology, as the empty sella may itself lead to enlargement of size.

Computed tomography (CT) is very helpful in the delineation of the osseous margins of the sella and in evaluation of the bony changes related to pathologic processes. Thin section 0.625 mm axial spirally acquired images can be reformatted into sagittal and coronal images.

MRI provides useful information about the relationship of the gland with adjacent anatomical structures. For the pituitary gland, thinner slices are acquired with smaller field of views centered at the sella. Dynamic contrast-enhanced sequences are obtained in the coronal plane and acquired every 30 seconds for 3 minutes following intravenous contrast injection. With recent advances, a variety of advanced MR techniques have been evolved which include 3D volumetric analysis of pituitary volume,high-resolution MR imaging at 3 Tesla (T) for evaluating pituitary stalk, diffusion-weighted imaging, MR spectroscopy, magnetization transfer ratio and intraoperative MRI. Post-gadolinium enhanced sequences are obtained with fat saturation to improve contrast between pathology and the basicranium. Proton MR spectroscopy is helpful in differentiating various lesions involving pituitary-hypothalamic axis.

Isotropic CISS and FIESTA-C are particularly useful for delineating the cisternal segments of the cranial nerves due to the bright signal from surrounding cerebrospinal fluid (CSF).

In characterisation of the lesions with MRI : the morphology, signal intensity, and contrast enhancement pattern are taken into consideration.

Although MRI is currently considered the examination of choice for sellar and parasellar pathologies due to its superior soft tissue contrast, multiplanar capability and lack of ionizing radiation, CT may be the only option in patients who cannot have an MRI examination (e.g. those with pacemakers, incompatible hardware and severe claustrophia).

The most recent advancement in pituitary imaging is the use of intraoperative MRI (IMRI) and intraoperative real-time ultrasonography which provides better visualization and facilitate complete resection of the tumor.

The major aim of this descriptive study is to enumerate in detail the various MR imaging characteristics of the tumors of the sellar, parasellar and suprasellar regions.

In the present study, most commonly mass lesions were encountered in 31-40 years age group patients. Females predominates present study constituting 60 % of the total study population.

These observations are in concordance with study done by Banna et al and *Batra V et al* [15][16]. In their prospective study they encountered maximum number of patients in fourth decade, and with female preponderance.

The most common mass lesion detected in our study was pituitary adenoma comprising 34% of the total cases. This is similar to the experience of Benjamin et al , Johnsen et al and *Batra V et al* [16][17][18][19].

PHYSIOLOGICAL CONDITIONS :

Pituitary hyperplasia is physiologic manifestation due to hypertrophy of prolactin cells during pregnancy or lactation and inhypofunctioning of the thyroid gland, adrenal glands, or gonads due to lack of negative feedback.

Ectopic neurohypophysis is a result of trauma or neoplastic processes. Septo-optic dysplasia is commonly associated with this condition. In pituitary stalk interruption syndrome, there is also an aplastic or hypoplastic infundibular stalk and adenohypophysis [20].

Empty sella is considered a common finding in imaging studies of the brain with a widely varying reported prevalence. It will demonstrate the sella to be filled with CSF and the infundibulum can be seen to traverse the space, thereby excluding a cystic mass. This is known as the infundibulum sign. Although the exact pathogenesis of primary ES is not known, it is postulated that a congenital defect/weakness in the diaphragm sellae coupled with CSF pulsation plays a major role (Fig.1).

NEOPLASTIC CONDITIONS :

Lipomas are congenital, benign fatty lesions often located at or near the midline. They may show calcifications and/or known to be traversed by blood vessels. On MRI, they appear isointense to subcutaneous fat on all sequences. Fat suppressed images are useful in distinguishing haemorrhagic or proteinaceous lesions.

Pituicytomas are also known as choristomas, granular cell tumors, or myoblastomasare usually seen in adults arising along the stalk and the posterior lobe. On MRI, characteristics vary depending on the cystic components. The solid parts of the tumor are usually enhancing.

Pituitary Adenoma

The classification of the adenomas has been done on the morphological size of the lesion as microadenomas (<10 mm) and macroadenomas (≥10 mm). Microadenomas may be difficult to detect due to their size but are highly symptomatic, while macroadenomas also exert mass effect. On MRI, immediately after contrast enhancement, microadenomas are hypointense on T1-weighted imaging relative to the remaining normal pituitary tissue. Dynamic contrast-enhanced MRI can further be performed to increase the sensitivity and specificity.

Macroadenomas are isointense to gray matter on T1- and T2-weighted imaging and demonstrate bright enhancement. Approximately, 10% of adenomas can show hemorrhage, infarction or necrosis/cystic change, which alters the MRI signal intensities (Fig.2).

Adenomas can also be classified according to their cellular origin into lactotrophs, somatotrophs, gonadotrophs, corticotrophs, and thyrotrophs.

In Dynamic studies, seven to ten images were obtained every 20 to 30 seconds while injecting gadolinium. The infundibulum and posterior lobe of pituitary gland are the first to show contrast enhancement at 20 seconds, followed by the anterior lobe from the junction of the infundibulum to the peripheral portion of the anterior lobe within 80 seconds after gadolinium injection. The pituitary adenomas show peak enhancement at 60 to 200 seconds after the most marked enhancements of the normal pituitary gland[21].

In pituitary apoplexy syndrome, patients present with ophthalmoplegia, headache, and visual loss due to pituitary infarction/ hemorrhage as a result of massive hemorrhage or tumor necrosis. Acute hemorrhage will appear hypointense on T2-weighted images with T1 hyperintensity as the hemorrhagic products evolve (Fig.3).

Meningioma

Parasellar meningiomas commonly involve the cavernous sinus, produce ophthalmoplegia, commonly occur along dural reflections and are almost always dural-based. Approximately 40% arise in the skull base [22].

On CT, they appear iso- to hyperdense to cerebral cortex and show calcifications or are associated with skull base hyperostosis (occurring in 50% of patients) compared to convexity meningiomas. On MRI, they are usually well circumscribed, isointense to slightly hypointense on T1, isointense to slightly hyperintense on T2 and they enhance homogenously and intensely, although this varies with degree of calcification or cystic degeneration (Fig.4). The vascular supply to these lesions is from the carotid meningeal and ophthalmic arteries.

Craniopharyngioma

Craniopharyngiomas are benign, non-glial epithelial tumors arising from remnants of Rathke's pouch or rests of buccal mucosa,along the trajectory of the craniopharyngeal duct. The main histologic subtypes are adamantinomatous, more commonly occuring in childhood as heterogeneous cystic and solid suprasellar masses and squamous papillary. More commonly occurring in adulthood as solid, less commonly calcified, and devoid of cysts. On MRI, solid components are hypointense on T1-weighted images and hyperintense on T2-

weighted images. The cysts also have a long T2 (Fig.5); however, if they have a high cholesterol content or methemoglobin, shortening of T1 results in high signal intensity on T1-weighted images. Craniopharyngiomacan cause truncation of the dorsum sellae and upward growth into the third ventricle. Papillary craniopharyngiomas and germinomas both usually show strong contrast enhancement, but germinomas have lower ADC values[23].

Chordoma and Chondrosarcoma

On CT, chondrosarcomas show osseous erosions and destructive changes usually with a calcified chondroid matrix[24]. On MRI, chondrosarcomas are usually well circumscribed and hyperintense on T2-weighted sequences, with variable degrees of heterogeneous contrast enhancement.

On MRI, chordomas are well circumscribed with a pseudoencapsulated appearance and markedly bright on T2-weighted sequences, probably secondary to mucin and/or necrosis.

Interlobular septa are formed by epithelioid cells and appear hypointenseon T2 with variable degrees of contrast enhancement. Chondrosarcomas have significantly higher ADC values than chordomas.

Schwannoma

Schwannomas are benign, well encapsulated, globular and slow-growing neoplasms that arise from Schwann cell; all of these features that distinguish them from broad-based meningiomas.

On MRI, schwannomas are iso- to hypointense on T1 and hyperintense on T2-weighted sequences although the heterogeneity varies according to the presence of cystic changes or, rarely, hemorrhage or calcifications and show avid contrast enhancement.

Optic Pathway and hypothalamic Glioma

They are commonly occuring optic nerve tumors with roughly one-third associated with neurofibromatosis type 1[25].

On MRI, there is fusiform and/or nodular enlargement of the optic chiasm and/or optic nerves with thickening of the third ventricular floor and hypothalamus. On MRI, they are iso- to hypointense on T1 and hyperintense on T2-weighted sequences (Fig.6). MRI is used in determination of infiltration of the optic chiasm or optic nerves and for assessing posterior extension into the lateral geniculate body and the occasional exophytic growth into the suprasellar and interpeduncular cisterns. Larger lesions may have cystic components and grow directly into the pituitary stalk.

Germ Cell Tumor

Extra-gonadal germ cell tumours include: germinoma (most common, approx. 50%-70%), mature teratoma, malignant teratoma, yolk sac tumour, embryonal carcinoma and choriocarcinoma. Alfa-fetoprotein and β-human chorionic gonadotropin are commonly found in CSF and serum and are helpful markers for diagnosis[26][27]. Germinomas are hyperdense on CT.The earliest finding of a suprasellar germinoma may be absence of the pituitary bright spot due to disruption of the infundibulo-neurohypophyseal system. On MRI, they are iso- to slightly hyperintense on T2-weighted images, and T1 signal intensity is variable. Germ cell tumors have a high propensity to seed CSF, and therefore imaging of the entire neuraxis is warranted.

The second most common germ cell tumors are teratoma. On MRI, they are relatively circumscribed lesions, with heterogeneous signal intensity on T1, T2WI and post-contrast sequences, with suppression of signal on fat-saturated imaging. Malignant tumors demonstrate marked enhancement. They may contain calcifications with low signal on T1 and T2WI.

Plasmacytoma

Plasma cell neoplasms may present as multiple myeloma or plasmacytomas.On MRI, they show intrinsic T1 hyperintensity presumably related to densely packed cells and a low water content. Plasmacytomas enhance avidly and homogeneously, which are also features of lymphoma, but the latter tends to have intermediate to low signal intensity on both T1 and T2-weighted sequences[28].

Metastases

The most common primaries in order of frequency are prostate and breast cancer, leukemias, lymphoma, and lung cancer[29]. Leptomeningeal metastases is seen with acute lymphoblastic leukaemia, medulloblastomas, germ-cell tumours, ependymomas and malignant gliomas[30].

On MRI, osseous metastases are hypointense geographic areas of marrow replacement on non-contrast T1-weighted sequences. Fat saturation is useful to visualize metastases after administration of intravenous contrast material. They may have a dumbbell morphology from invasion through the diaphragmasella. Diffusion-weighted imaging detects calvarial metastases as areas of increased marrow signal, with the exception of prostate cancer, which is primarily sclerotic[31][32].

CONGENITAL CONDITONS:

Rathke Cleft Cyst

These are benign, true epithelial cysts believed to arise from remnants of Rathke's pouch due to incomplete obliteration of the embryonic cleft. On MRI, they are frequently hyperintense on T2-weighted images, lesions that are homogeneously T2 hypointenseare highly suggestive of the diagnosis, as is the presence of a T1-hyperintense and T2-hypointense intracystic nodule which represents a mucinous mass with cholesterol and protein. There is no contrast enhancement centrally; however, occasionally there may be a thin peripheral rim of enhancement from associated inflammation. This feature helps distinguish these lesions from craniopharyngiomas.

Dermoid and Epidermoid Tumor (congenital cholesteatoma)

Dermoids and epidermoids are both non-neoplastic lesions developing from inclusion of ectodermal remnants during neural tube closure and differ histopathologically in that dermoids contain dermal appendages and epidermoids do not[33][34].

On CT, most epidermoids are hypo-dense and are difficult to distinguish from arachnoid cysts.

Few lesions show increased density as a result from hemorrhage, increased protein, or saponification. On MRI, their T1 and T2 signal intensities are usually close to those

of CSF, but the lesion does not suppress on fluid-attenuated inversion recovery (FLAIR) sequences, on which it shows a “dirty” appearance. Classically, they demonstrate very high (“light bulb bright”) signal intensity on diffusion weighted sequences, with ADC values that may not be as low as expected.

Dermoids tend to follow fat characteristics on CT and MRI but may be hypointense on T2. Fluid/fluid or fluid/debris levels may be present.

Arachnoid Cyst

Arachnoid cysts are benign non-neoplastic structures filled with CSF and lined by arachnoid cells and collagen. Most arachnoid cysts follow CSF signal intensity i.e. low signal intensity on T1WI, FLAIR and DWI, high signal intensity on T2WI with no contrast enhancement, except for some that may contain increased proteins or hemorrhage[35].

Hypothalamic Hamartoma

Hamartoma of the tuber cinereumis a developmental heterotopia, which usually presents in childhood. On MRI, they are mildly hyperintense on T2 (probably due to glial tissue) and iso- to hypointense on T1-weighted sequences. They can be distinguishes from hypothalamic gliomas and germinomas as they show no contrast enhancement or restricted diffusion[36].

VASCULAR CONDITIONS:

Numerous vascular malformations can be seen in the sellar/juxtasellar regions namely arterial aneurysms (saccular or giant aneurysms of the internal carotid artery), cavernous carotid fistulas, arterial-venous malformations, haemangiomas or cavernous malformations.

Giant aneurysm

Giant aneurysms are greater usually than 25 mm in diameter. On MRI, they appear as single or multiple multilobulated intra-axial lesions with a peripheral or irregular zone of low signal on T2WI secondary to haemosiderin, with a central zone of variable signal on T1WI and T2WI depending on ages of haemorrhagic components. Contrast enhancement is usually absent. Magnetic resonance angiography (MRA) is useful in confirming an aneurysm.

Carotid-cavernous fistula

The fistulous communication between the carotid artery and cavernous sinus usually is a result of a dural arteriovenous malformation, trauma or transsphenoidal surgery. Parasellar and orbital veins show flow effects and flow artifacts on MRI.

INFLAMMATORY/GRANULOMATOUS CONDITIONS:

Sarcoidosis

Systemic sarcoidosis is seen involving any part of the brain, meninges, cranial nerves, or calvarium with leptomeningeal or pachymeningeal thickening and enhancement and/or cerebral or soft tissue granulomata. On MRI, sarcoid lesions are hypointense on T2-weighted images but this finding remains nonspecific.

Lymphocytic Hypophysitis

Lymphocytic hypophysitis is an infiltrative autoimmune/ inflammatory disorder which affects the anterior or posterior pituitary gland or infundibulum commonly in pregnant or postpartum patients and autoimmune conditions, including drug related (eg : ipilimumab). On MRI, it shows intermediate signal on T1WI, heterogeneous low-intermediate and high signal on T2WI involving the pituitary lobe with thickened pituitary stalk, and prominent homogeneous or heterogeneous post contrast enhancement. A characteristic finding includes a parasellar T2 dark sign, which helps in determining lymphocytic hypophysitis from a pituitary adenoma.

INFECTIOUS CONDITIONS :

Pituitary abscesses can occur as sequelae of sepsis, extension of sinusitis, sphenoid osteomyelitis, cavernous sinus thrombophlebitis and meningitis. On MRI, the features are of a cystic lesion with iso- or hypointense signal on T1W images and iso- or hyperintense signal on T2W images (Fig.7). After gadolinium administration, the lesion demonstrates heterogeneous peripheral enhancement.

CONCLUSION:

MRI is useful in diagnosing sellar, parasellar and suprasellar lesions with high accuracy, sensitivity and specificity. There is better visualization of the morphology of lesions, nature of contrast enhancement and extent of lesions. Hence, we have briefly discussed the imaging characteristics of various sellar, parasellar and suprasellar lesions. A detailed knowledge of the sellar, parasellar and suprasellar anatomy aids in improvement in the interpretation of the images, leading to reduced errors and increased diagnostic value in reporting.

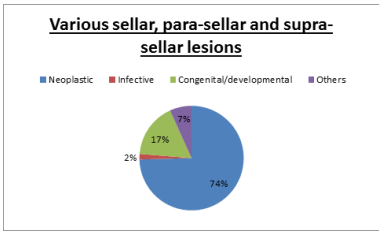

Chart 1: Various sellar, para-sellar and supra-sellar lesions.

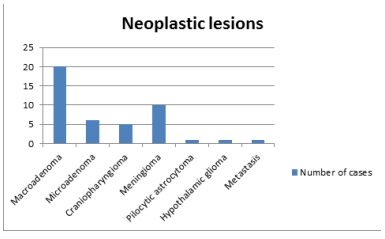

Chart 2: Types of neoplastic lesions.

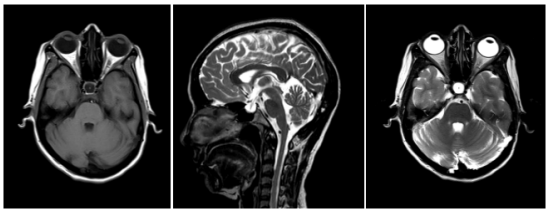

Figure 1: In this case of Empty sella, most of the sella turcica is occupied by cerebrospinal fluid, which appears hypointense on T1WI and hyperintense on T2WI.

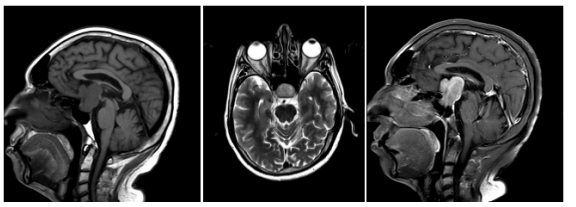

Figure 2: In this case of Pituitary macroadenoma, there is a solid enhancing lesion in the suprasellar region which appears isointense on both T1WI and T2WI, also causing widening of the pituitary fossa. On post contrast administration, the lesion shows bright enhancement.

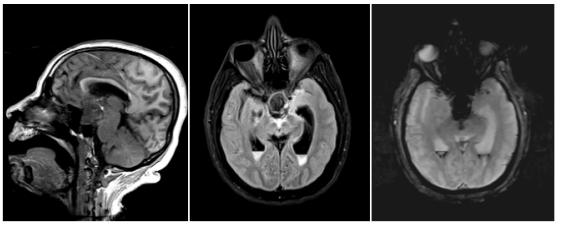

Figure 3: In this case of Pituitary apoplexy, there is an area of hemorrhage within the adenoma which appears heterogeneous on both T1WI and T2WI with blooming on GRE sequence. There is extension of bleed into bilateral lateral ventricles.

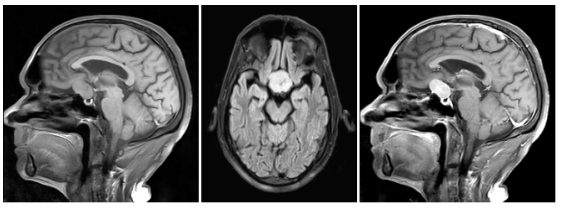

Figure 4: In this case of meningioma, there is a well-circumscribed extraaxial suprasellar lesion appearing isointense on T1WI and slightly hyperintense on T2WI showing homogeneous enhancement on post contrast administered T1WI.

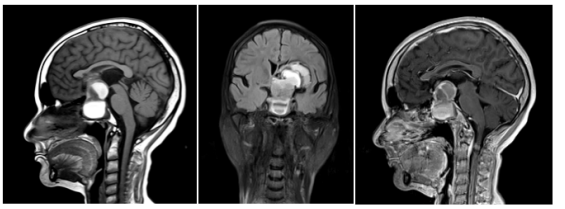

Figure 5 : In this case of craniopharyngioma there is a heterogeneous intensity solid cystic suprasellar lesion with solid component showing mild enhancement on post contrast T1WI.

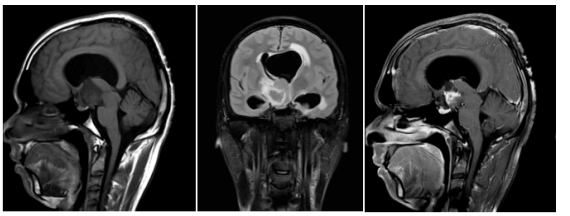

Figure 6: In this case of hypothalamic glioma, there is a heterogeneously enhancing lesion arising from the floor of the 3rd ventricle and the hypothalamus.

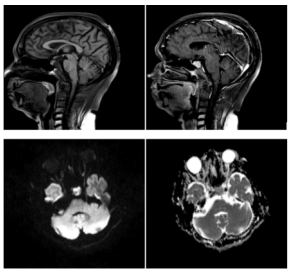

Figure 7: In this case of pituitary abscess, there is a heterogeneously enhancing T1 hypointense sellar lesion showing subtle diffusion restriction.

REFERENCES

1. Ruscalleda J. Imaging of parasellar lesions. European Radiology. 2005;15:549-59.
2. Davis PC, Hoffmann JC et al. Gadolinium DTPA and MR imaging of pituitary adenoma: a preliminary report. AJNR 1987; 8:817-823
3. Delman BN (2009) Imaging of pediatric pituitary abnormalities. Endocrinol Metab Clin N Am 38:673–698
4. Kollias SS, Ball WS, Prenger EC. Review of the embryologic development of the pituitary gland and report of a case of hypophyseal duplication detected by MRI. Neuroradiology. 1995;37(1):3-12.
5. Ikeda H, Suzuki J, Sasano N,Niizuma H. The development and morphogenesis of the human pituitary gland. Anat Embryol (Berl). 1988;178(4):327-336.
6. Crenshaw WB, Chew FS. Rathke's cleft cyst. AJR Am J entgenol. 1993;158:1312. [PubMed]
7. Schwartzberg DG. Imaging of pituitary gland tumors. Semin Ultrasound CT MR. 1992;13:207–23.[PubMed]
8. Kiortsis D, Xydis V, Drougia AG et al (2004) The height of the pituitary in preterm infants during the first 2 years of life: An MRI study. Neuroradiology 46:224–226
9. Delman BN (2009) Imaging of pediatric pituitary abnormalities. Endocrinol Metab Clin N Am 38:673–698
10. Elster AD. Imaging of the sella: Anatomy and pathology. Semin Ultrasound CT MR. 1993;14:182–94.[PubMed]
11. Carpenter MC. 2nd ed. Baltimore, MD: Williams and Wilkins; 1978. Core text of neuroanatomy; pp. 216–35.
12. Dietrich RB, Lis LE, Greensite FS, Pitt D (1995) Normal MR appearance of the pituitary gland in the first 2 years of life. AJNR Am J Neuroradiol 16:1413–1419
13. Colombo N, Berry I, Kucharczyk J, Kucharczyk W, de Groot J, Larson T, et al. Posterior pituitary gland: Appearance on MR imaging in normal and pathological states. Radiology. 1987;165:481–5.[PubMed]
14. Sato N, Ishizaka H, Yagi H, Matsumoto M, Endo K. Posterior lobe of the pituitary in diabetes incipidus: Dynamic MR imaging. Radiology. 1993;186:357–60. [PubMed]
15. Banna M, Baker HL, Houser OW. Pituitary and parapituitary tumours on computed tomography. BJR. 1980;53:1123-43.
16. Batra V et al. Int J Res Med Sci. 2016 Sep;4(9):3924-3928 www.msjonline.org pISSN 2320-6071 | eISSN 2320-6012
17. Lee BCP, Deck MDF. Sellar and juxtasellar lesion detection with MR. Radiology. 1985;157:143-7.
18. Johnson DE, Woodruff WW, Allen IS, Cera PJ, Funkbouser GR, Coleman LL. MR imaging of sellar and juxtasellar regions. Radiographics. 1991:11:727-58.
19. Taylor SL, Barakos JA, Harsh GR 4th, Wilson CB. Magnetic resonance imaging of tuberculum sellae meningiomas: preventing preoperative misdiagnosis as pituitary macroadenoma. Neurosurgery. 1992;31(4):621-7.
20. Schubiger O, Haller D. Metastases to the pituitary-hypothalamic axis: An MR study of 7 symptomatic patients. Neuroradiology. 1992;34(2):131-134.
49. 21. Sakamoto Y, Takahashi M, Korogi Y, Bussakhi H, Ushio Y. Normal and abnormal pituitary glands: gadopentate dimeglumine enhanced MR imaging. Radiology 1997; 178:441- 445
22. Schick U, Hassler W. Surgical management of tuberculum sellae meningiomas: involvement of the optic canal and visual outcome. J Neurol Neurosurg Psychiatry.2005;76(7):977-983.
23. Lee HJ,Wu CC,Wu HM, et al. Pretreatment diagnosis of suprasellar papillary craniopharyngioma and germ cell tumors of adult patients. Am J Neuroradiol. 2015;36(3):508-517.
24. Lee YY, Van Tassel P. Craniofacial chondrosarcomas: imaging findings in 15 untreated cases. Am J Neuroradiol. 1989;10(1):165-170.
25. Dutton JJ. Gliomas of the anterior visual pathway. Surv Ophthalmol. 1994;38(5):427-452.
26. Echevarria ME, Fangusaro J, Goldman S. Pediatric central nervous system germ cell tumors: a review. Oncologist. 2008;13(6):690-699.
27. Packer RJ, Cohen BH, Cooney K. Intracranial germ cell tumors. Oncologist. 2000;5(4):312-320.
28. Huang BY, Castillo M. Nonadenomatous tumors of the pituitary and sella turcica. TMRI. 2005;16(4):289-299.
29. Laigle-Donadey F, Taillibert S, Martin-Duverneuil N, Hildebrand J, DelattreJY. Skull-base metastases. J Neurooncol. 2005;75(1):63-69.
30. Chamberlain MC (1995) A review of leptomeningeal metastases inpediatrics. J Child Neurol 10:191–199
31. Ginat DT, Mangla R, Yeaney G, Ekholm S. Diffusion-weighted imaging of skull lesions. J Neurol Surg B Skull Base. 2014;75(3):204-213.
32. Nemeth AJ, Henson JW,Mullins ME, Gonzalez RG, Schaefer PW. Improved detection of skull metastasis with diffusion-weighted MR imaging. Am J Neuroradiol. 2007;28(6):1088-1092.
33. Caldarelli M, Massimi L, Kondageski C, Di Rocco C. Intracranial midline dermoid and epidermoid cysts in children. J Neurosurg. 2004;100(5 suppl Pediatrics):473-480.
34. Orakcioglu B, Halatsch ME, Fortunati M, Unterberg A, Yonekawa Y. Intracranial dermoid cysts: variations of radiological and clinical features. ActaNeurochir (Wien). 2008;150(12):1227-1234; discussion 1234.
35. Osborn AG, Preece MT. Intracranial cysts: radiologic-pathologic correlation and imaging approach. Radiology. 2006;239(3):650-664.
36. Choi IS, David C. Giant intracranial aneurysms: development, clinical presentation and treatment. Eur J Radiol. 2003;46(3):178-194.